scientific reports

Check for updates

OPEN

Dynamics of detergent-resistant membranes of *Plasmodium falciparum* during blood stage development

Gabriella Sferra[1,4,5], Federica Fratini[2,5], Cecilia Birago[1], Laura Megliorini[2], Stefania Mochi[1], Marco Lalle[1], Silvio Paone[1], Anna Olivieri[1], Carla Ferreri[3], Anna Sansone[3], Marta Ponzi[1], Chiara Currà[1,5]✉ & Elisabetta Pizzi[2,5]

Membrane microdomains, also known as detergent-resistant membranes (DRMs), are tightly packed assemblies enriched in cholesterol and sphingolipids, where various membrane-associated processes occur. Many intracellular pathogens, including *Plasmodium*, exploit these raft-like structures to recognize and invade host cells. In particular, *Plasmodium* depends on host cholesterol to build its own membranes, as it is unable to perform sterol synthesis. Using quantitative proteomics, lipid analysis, and bioinformatics, this study defines the composition and dynamics of *Plasmodium falciparum* DRMs from key developmental stages: schizonts, which give rise to invasive merozoites, and gametocytes, which are responsible for transmission to the mosquito vector. Comparative analysis of the flotation properties of DRM-associated proteins and lipids reveals both conserved and stage-specific features in the structural organization of membrane microdomains. Following parasite invasion, host DRMs are also remodeled with the internalization of components of the erythrocyte junctional complex and their repositioning in the newly generated parasitophorous vacuole membrane. Prediction and analysis of the DRM interactomes reveals a core of proteins involved in fundamental biological processes maintained between the schizont and gametocyte stages. This common core forms a highly interconnected subnetwork that occupies a central position in the interactomes, while stage-specific functions occupy a peripheral position in the network.

Keywords Malaria parasite, *Plasmodium falciparum*, Lipid rafts, Protein-protein interaction networks, Proteomics, Lipid analysis

Abbreviations

DRM	Detergent-resistant membrane
DSM	Detergent-soluble membranes
FDR	Discovery rate
GC	Gas chromatography
GPI	Glycosylphosphatidylinositol
HPTLC	High-performance thin-layer chromatography
IFA	Indirect immunofluorescence assay
LFQ	Label-free quantification
MC	Maurer's clefts
MßCD	Methyl-ß-cyclodextrin
PV	Parasitophorous vacuole
PAP	Protein abundance profile
PPI	Protein-protein interaction
PVM	PV membrane
RBC	Red blood cell

[1]Department of Infectious Diseases, Istituto Superiore di Sanità, Roma, Italy. [2]Core facilities Technical-scientific service, Istituto Superiore di Sanità, Roma, Italy. [3]Consiglio Nazionale delle Ricerche, ISOF, Bologna, Italy. [4]Present address: Department of Bioscience and Territory, University of Molise, Campobasso, Italy. [5]Gabriella Sferra, Federica Fratini, Chiara Currà and Elisabetta Pizzi contributed equally to this work. ✉email: chiara.curra@iss.it

iRBCs Infected RBCs

The complex life cycle of the intracellular malaria parasite involves a mosquito vector of the genus *Anopheles* and a vertebrate host. The invasive sporozoites, injected by an infected mosquito, hide inside liver hepatocytes producing thousands of merozoites that invade circulating red blood cells (RBCs), thus triggering the symptomatic phase of malaria infection. The deadliest human parasite, *Plasmodium falciparum*, completes an asexual blood cycle in about 48 h. An infective merozoite contacts and penetrates the host cell via receptor binding. Parasite invasion ligands are secreted onto the merozoite apical end from specialized organelles, the micronemes, and the anterior necks of rhoptries. Upon attachment, the merozoite forms a tight junction that seals the host and parasite plasma membranes. RBC penetration is powered by a unique, substrate-dependent, gliding motility machinery (glideosome), an actomyosin complex that underlies the plasma membrane. During host cell entry, the parasite discharges rhoptry proteins and lipids, and the RBC membrane invaginates, promoting the formation of a parasitophorous vacuole (PV) that houses the parasite during the entire blood stage development and replication. A new generation of invasive merozoites is formed and released by the successive rupture of the PV membrane (PVM) and the host plasma membrane[1,2].

Most blood-stage parasites replicate by schizogony, generating a multinucleate syncytium (schizont), while a small fraction commits to sexual stage differentiation (gametocytogenesis), which leads to the production of male and female gametocytes. These gamete precursors ensure parasite transmission to the mosquito vector. In *P. falciparum*, gametocyte maturation occurs in about ten days, passing through five morphologically distinct stages (I-V).

Asexual trophozoite and schizont, as well as immature gametocyte stages are sequestered in the internal organs of the human host. In contrast, mature stage V gametocytes circulate in the peripheral blood to be picked up by a mosquito vector.

In the mosquito midgut, gametocytes undergo gametogenesis to form male and female gametes. Female gametocytes produce a single macrogamete, while male gametocytes replicate their genome three times to produce eight flagellated microgametes. For mating to occur, both male and female gametes egress from the host erythrocyte with an inside-out process involving the successive rupture of the PVM and the RBC plasma membranes. In about 24 h, the zygote transforms into a motile ookinete that traverses the midgut wall to encyst and replicate, resulting in thousands of sporozoites. This motile form migrates to the salivary glands to be injected into a new vertebrate host.

Asexual and sexual blood stages undergo morphological changes to face different environmental challenges; these include an extensive remodeling of the host erythrocytes, with the generation of new membrane compartments such as the PVM or cisternae-like organelles anchored to the erythrocyte cytoskeleton. Previous studies identified cholesterol-rich membrane microdomains (also known as lipid rafts) in membranous structures of parasite origin, such as the PVM[3,4] and the so-called Maurer's clefts (MC) that mediate protein trafficking from parasite to host cell cytosol and plasma membrane[3]. These membrane assemblies were also identified in the rhoptries and micronemes, secretory organelles of the invasive merozoites[5].

Membrane microdomains, detected in all cell types, are tightly packed assemblies enriched in cholesterol and sphingolipids and preferentially associated with GPI-anchored or acylated proteins resulting in liquid-ordered structures embedded in a fluid membrane environment[6]. The chemo-physical properties of these liquid-ordered compartments make them resistant to cold non-ionic detergents. In general, detergent-resistant membranes (DRMs), isolated from the bulk cell membrane, reflect the intrinsic affinity of a protein for the ordered state of the membrane, characteristic of rafts[7].

This unique structural organization serves as a platform where selected protein-protein or lipid-proteins interactions occur, thus favoring the compartmentalization of diverse membrane-associated processes such as signal transduction, which regulates several cellular pathways, endocytosis, and protein trafficking[8]. In addition, many pathogens exploit lipid rafts for host cell recognition and internalization[9].

These membrane assemblies have a crucial role in various aspects of the endocellular life cycle of malaria parasite. Cholesterol depletion by methyl-ß-cyclodextrin (MßCD) inhibits parasite invasion and growth. At the trophozoite stage, MßCD treatment produces a collapse of the complex membrane network inside the infected RBCs with expulsion of trophic stages[10]. Further, invasion is inhibited when RBCs are treated with lidocaine, a local anesthetic, which disrupts lipid rafts reversibly without removing membrane cholesterol[11]. Thus, altered lipid/protein composition of membrane rafts may lead to changes in their functional properties.

Interestingly, *Plasmodium* lacks the ability to synthesize cholesterol *de* novo[12] suggesting a complete dependence on host cholesterol with mechanisms still not completely elucidated. A novel membrane transport system was postulated between PV and RBC membranes devoted to cholesterol import[13].

Because of the crucial role of membrane microdomains in *Plasmodium* biology and virulence, there is growing interest in defining the compositional heterogeneity of these assemblies and their dynamics in physiological and pathological conditions.

In this study, we compared the lipid and protein composition of DRMs of RBCs infected with two highly specialized blood stages of the human parasite *Plasmodium falciparum*: the schizont stage, in which invasive merozoites are formed and the gametocytes responsible for transmission to the mosquito vector. Stage-related DRMs were investigated by quantitative proteomics, lipid analysis, and statistical approaches. Based on the flotation profiles of proteins and lipids associated with DRMs, we describe the stage-specific organization of these membrane assemblies, their composition and compartmentalization. Comparative analysis of the stage-related interactomes of DRMs reveals a common core of highly interconnected proteins involved in fundamental biological processes. In contrast, stage-specific functions are less connected to the rest of the network and occupy a peripheral position in both asexual and sexual stages.

Overall, our results suggest that the spatial compartmentalization conferred by DRM organization is likely necessary for the proper execution of complex processes such as human host cell invasion and egress, cellular trafficking, nuclear activities, and mosquito colonization. This body of data may provide insights for the development of yet unexplored intervention strategies.

Results

Protein and lipid composition of DRMs in asexual and sexual blood stages of *P. falciparum*

DRMs of the asexual stages of *P. falciparum* were prepared from early schizonts, about 36 h post-invasion (hpi), and from late schizonts (segmenters) with fully formed merozoites, about 46 hpi. Sexual stage DRMs were prepared from gametocytes, stage IV/V, about 9/10 days post-induction. Free vacuolar parasites, recovered by low-speed centrifugation after osmotic lysis, were treated with cold Triton-X100 to dissolve the bulk of the membranes, while retaining detergent-resistant, cholesterol-rich microdomains. These were isolated by sucrose gradient centrifugation, exploiting their flotation properties. DRM containing fractions 2–8 were collected and analyzed in biological replicates to identify and robustly quantify the protein components by mass spectrometry (three biological replicates, supplemental Tables S1-S3) or saturated and unsaturated fatty acids, by gas chromatography (two biological replicates, supplemental Table S4).

In total, we identified 216 DRM-associated proteins in early schizonts, 292 in late schizonts, and 121 in gametocytes, including proteins detected in a single replicate, with a minimum of two distinct peptides (Fig. 1A and Supplemental Table S5). More than 70% of proteins were identified in at least two out of the three biological replicates (Supplemental data and Tables S1-S3). 74% of the DRM proteome of early schizonts is in common with that of late schizonts, while 67% of the DRM proteome of gametocytes is included in that of early or late schizonts or both. A DRM core of 70 proteins is shared by the three developmental stages (Fig. 1A). These include proteins involved in fundamental processes such as metabolism, protein trafficking, folding, or nuclear activities (Fig. 1B and Table S5A).

Based on the analysis of large-scale datasets in PlasmoDB (https://plasmodb.org, Release 68, May 2024), 19.9% of DRM-associated proteins in early schizonts and 23.3% in late schizonts contain a predicted signal peptide, twice as much as predicted in the total parasite proteome (11.33%). In gametocytes, this percentage reaches 30% of DRM-associated proteins, suggesting that these assemblies are strongly implicated in membrane trafficking. Furthermore, comparative analysis with a study that predicts the subcellular localization of the entire proteome of asexual stages[14] suggests that cholesterol-rich microdomains of parasite origin may reside in different membrane compartments, the PVM, the erythrocyte membrane, or membranous structures within the parasite (Table S5A).

As mentioned above, the asexual and sexual stages share a subset of DRM-associated proteins, some of which are involved in protein trafficking and folding. These include two signal peptide-containing proteins, the thioredoxin-like PF3D7_1104400 with a role in the invasion of RBCs, localized in the apical portion of merozoites as well as in the PVM of trophozoites[15] and the PV-resident protein P113 PF3D7_1420700 [16], which interacts with the PVM-associated export complexes PTEX (*Plasmodium* translocon of exported proteins)[17] and EPIC (exported protein-interacting complex)[18]. Both proteins were detected in the DRM fraction of *P. falciparum* asexual stages[3,5].

Here, we asked whether their subcellular localization is also maintained in gametocytes. In young gametocytes, validated antibodies against the thioredoxin-like and P113 proteins[3] decorated the parasite periphery, consistent with a localization in the PVM, while in late gametocytes (stage IV/V) they recognize vesicle-like structures exported to the cytoplasm and periphery of the infected erythrocyte (Figure S1).

Asexual and sexual DRM proteomes also include proteins participating in stage-specific processes (Fig. 1B, Table S5A). For example, DNA replication licensing factors were identified exclusively in early schizonts, when the parasite begins to multiply. In contrast, most of the proteins involved in the invasion process were identified only in DRMs of late schizonts.

In gametocyte DRM proteome, we identified two members of the PHIST family (Plasmodium helical interspersed subtelomeric family)[19] exported to the host cell compartment, PF3D7_0424600 and PF3D7_1102500 also known as PfGEXP02 that have been shown to interact with iRBC cytoskeleton[20]. However, most proteins specifically identified in gametocyte DRMs participate in processes that occur later in the mosquito midgut: the release of gametes from the host RBC and mating.

Because both lipids and proteins contribute to the distinct chemo-physical properties of membrane microdomains and their flotation capacity, we determined fatty acid composition: saturated, monounsaturated, and polyunsaturated ω3 and ω6, in each of the gradient fractions 2–8 (Table S4). As shown in Fig. 1C, the abundance of fatty acid types was expressed as a percentage; lighter fractions 2–6 are characterized by membranes with a higher percentage of saturated fatty acids (60–70% of total) and lower percentage of monounsaturated and polyunsaturated fatty acids, consistent with chemo-physical properties of liquid-ordered membranes. At difference, a marked decrease of saturated fatty acids (SFAs) was observed in fractions 7–8, balanced by an increase of PUFAs. This could account for decreased flotation capacity, probably due to increased sensitivity to solubilization by non-ionic detergents.

As previously observed in *P. berghei*[21] sexual stage DRMs of *P. falciparum* are characterized by an unexpectedly high content of ω3 polyunsaturated fatty acids, suggesting that the structural organization of gametocyte DRMs may differ from that of asexual stages.

These preliminary observations indicate that DRM-associated proteins are involved in general processes, such as secretion, transport, membrane fusions, or nuclear activities shared by different blood stages as well as in stage-specific functions, such as host cell invasion or gamete egress and fertilization. Further, DRMs are structural constituents of intracellular organelles and membrane structures exported to the host erythrocyte.

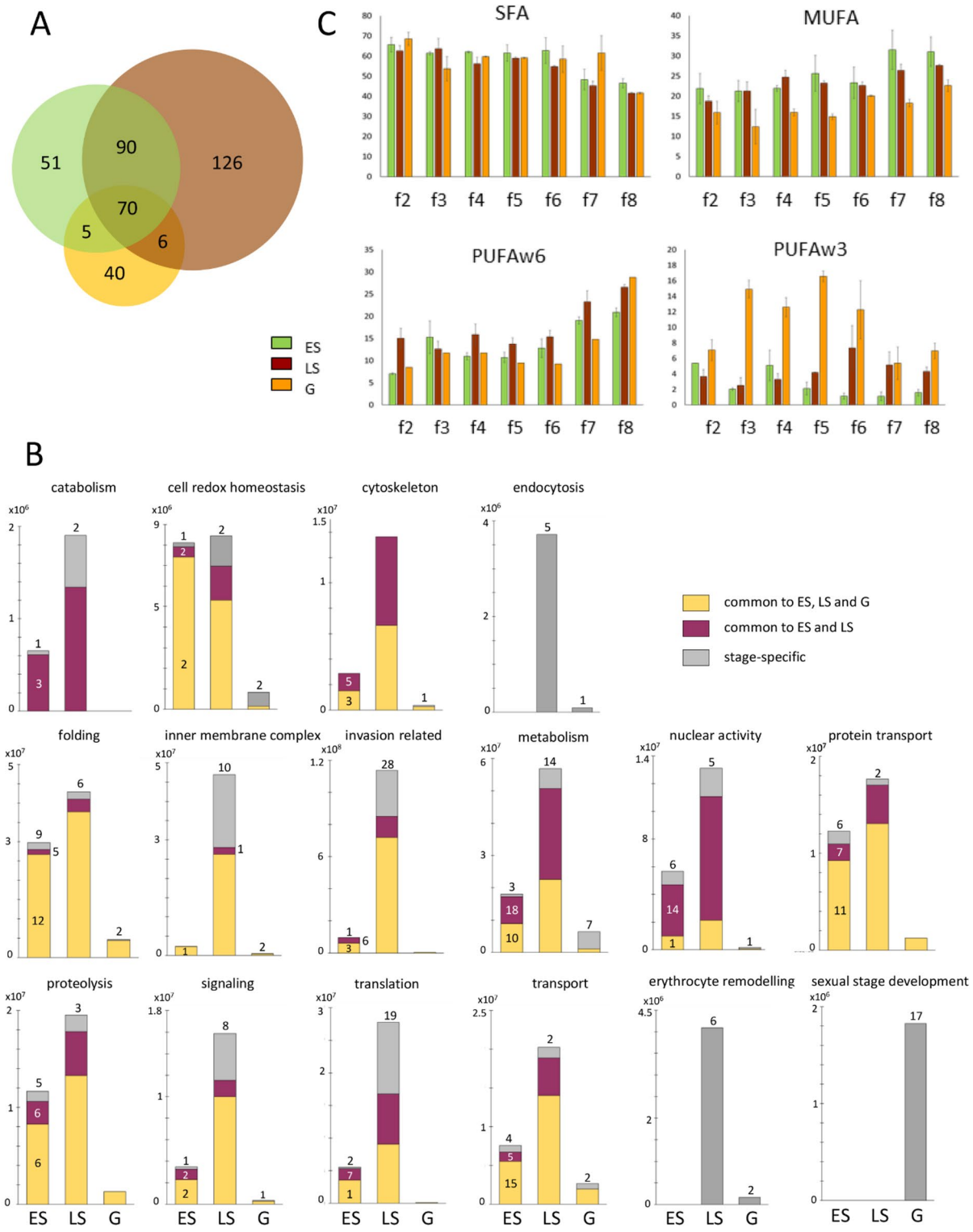

Fig. 1. Organization of *P. falciparum* DRMs in asexual and sexual stages. (**A**) Venn diagram of DRM-associated proteins identified in early schizonts (ES) and late schizonts (LS) and gametocytes (G) of *P. falciparum*; (**B**) Per each functional category, the abundance of proteins is subdivided in proteins common to all stages (ES, LS, and G), common to asexual stages (ES and LS) and stage specific proteins; the number of proteins in each class is also reported. (**C**) DRM lipids in gradient fractions 2–8 of the three stages ES, LS and G were analyzed by gas chromatography to determine relative abundances of fatty acids: saturated (SFA), monounsaturated (MFA), polyunsaturated omega6 (PUFAw6) and omega3 (PUFAw3).

Flotation properties of stage-related DRMs

To study the organization of stage-related DRM proteomes we constructed a flotation profile of each DRM-associated protein (PAP)[21] based on its abundance in gradient fractions 2–8, determined by label free quantification (LFQ) (Top3). Pre-processing of the data and assessment of PAP reproducibility (supplemental material) indicate that more than 70% of the proteins have well superimposable PAPs in at least two out of three replicates ($R > 0.55$, $P < 0.05$). This set was considered as an internal control of the robustness of the adopted procedure, consistent with a previous study[21]. The higher variability of the remaining PAPs could be explained by the inherent characteristics of some microdomains, which are more susceptible to detergent extraction probably because of their less ordered organization.

To compare the PAPs of stage-related proteomes we first constructed "reference" profiles using the mean abundance value of each protein in the three replicates. The reference PAPs of the three stages were then subjected to cluster analysis altogether. 6 clusters (P1-P6) were identified as representative of flotation profiles (Fig. 2A): clusters P1-P3 comprise raft-like, liquid ordered microdomains, with proteins floating in the lighter fractions 3–6; cluster 4, proteins with more complex profiles, probably shared by microdomains with different flotation properties, and P5 and P6, proteins floating in the heavier fractions 7 and/or 8, likely residing in microdomains more sensitive to detergent treatment.

As shown in Fig. 2B, proteins recruited into raft-like microdomains account for 23% in early schizonts, 48% in late schizonts and 36% in gametocytes, while proteins recruited into less ordered microdomains account for 54% of DRM-associated proteins in early schizont, 30% in late schizonts and 51% in gametocytes.

This percentage varies also among functional categories (Fig. 2C). For example, about 20% of proteins involved in cell redox homeostasis reside in raft-like microdomains in early schizonts; these percentage rises to 70% in mature schizonts, whereas proteins assigned to this category reside in less ordered domains in gametocytes.

Interaction networks of DRM-associated proteins in asexual and sexual blood stages

To study protein interactions in these distinct highly dynamic membrane compartments, we constructed a global *P. falciparum* interactome. A protein-protein interaction network was inferred using a Bayesian approach[22] based on the analysis of genomic and transcriptomic data available in PlasmoDB. From these data, we derived three new datasets: phylogenetic profile, gene expression profile, and rosetta-stone (detailed in supplemental material).

We used distance correlation as similarity metric because it increases the predictive performance of the phylogenetic profiles[23]. Expression profiles were constructed using microarray data from two different experiments[24,25]. We included the expression data from both asexual and sexual stages, as the latter are not present in the available protein-protein interaction networks[26].

The predicted global interactome includes 4805 proteins linked by 403,239 edges representing all possible protein interactions regardless of their sub-cellular localization, stage specificity and temporal co-presence. To take into account spatial and temporal variables, the global interactome was then filtered to keep connections of proteins identified in DRM proteome of early schizonts (185 proteins; 1036 edges), late schizonts (261 proteins; 2067 edges) and gametocytes (97 proteins; 329 edges) thus generating three stage-related interactomes (Fig. 3).

Functional categories were mapped on the three interactomes and their distinct organization was described by the topological parameters, the clustering coefficient, and the closeness, normalized on the mean value of the total nodes of the network (Fig. 3). In the interactome of early and late schizonts, clustering coefficient analysis indicates that proteins involved in the same process are organized in clusters except for proteins participating to nuclear activities, cytoskeleton organization, and inner membrane complex. Based on closeness values, stage-specific functions related to motility and invasion are peripherally located, with nodes poorly interconnected with the rest of the network. In contrast, general processes such as nuclear activities, folding, or translation occupy a central position. In gametocyte interactome, proteins involved in folding and sexual stage development are organized in clusters. As in the case of schizonts, stage-specific functions occupy a peripheral position in the network. Furthermore, comparative analysis (DyNet tools in CytoScape 3.10.1)[27] shows that 55 out of 70 proteins shared by the three DRM proteomes are mapped in the interactomes. These include proteins involved in folding, metabolism, protein transport and transport (Additional data) and form a highly interconnected subnetwork (Figure S2) suggesting the presence of a common scaffold of DRM-associated processes.

Dynamics of DRM recruitment in erythrocytes infected by asexual blood stages

The availability of trophozoite proteome[28] together with DRM proteomes from trophozoites[3] early and late schizonts (this study), allowed us to apply a comparative approach to investigate time of expression and dynamics of protein recruitment in DRMs (Table S5B and Table 1). Proteins expressed from trophozoites to mature schizonts and stably residing in DRMs, are mainly involved in cell redox homeostasis, transport, protein trafficking, metabolism, folding, and proteolysis. More than 50% of proteins with a role in nuclear processes are expressed at the trophozoite stage but recruited to DRMs during schizogony. Interestingly, DNA replication licensing factors are expressed at the trophozoite stage but detected in membrane microdomains exclusively in the early stages of schizogony, when DNA replication occurs (Table S5B). In addition, about 80% of the constituents of the inner membrane complex/gliding motility and about 50% of the invasion-related proteins are expressed at the trophozoite stage but translocated into the DRMs only in late schizonts.

About half of the DRM-associated proteins in early and late schizonts share similar flotation properties (Table S5A). When considering functional categories, this percentage rises to more than 70% in folding, protein transport, proteolysis and signaling, while most proteins reside in different DRM contexts when considering cell redox and nuclear activity categories (Table 2 and Table S5A).

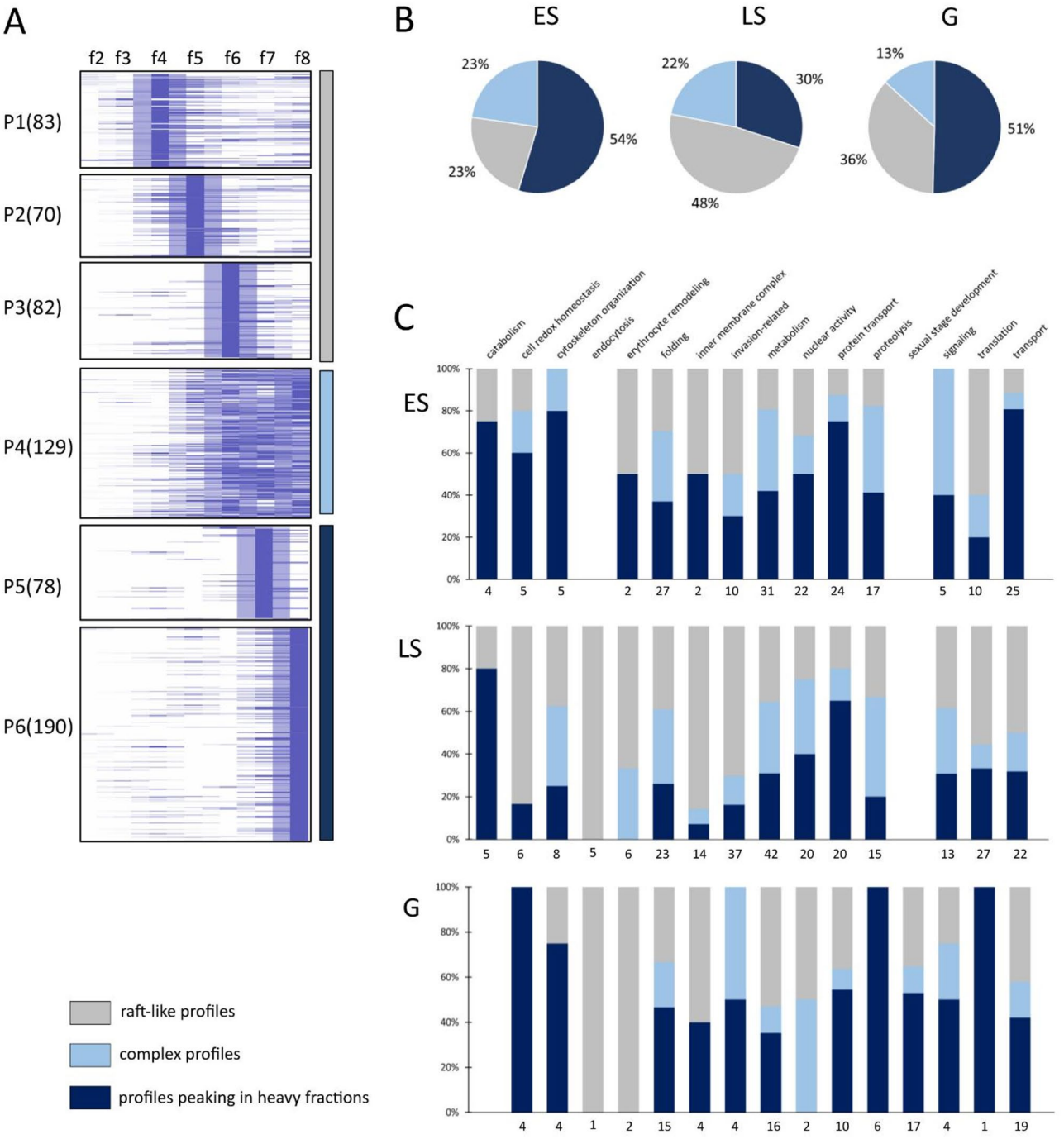

Fig. 2. Analysis of flotation properties of *P. falciparum* blood stage DRMs. (**A**) K-means clustering of protein abundance profiles (PAPs) of early schizont (ES), late schizonts (LS) and gametocytes (G) identified 6 clusters P1-P6 (similarity metric = Pearsons correlation coefficient); the number of proteins that fall in each cluster is indicated in parenthesis. Clusters were further grouped in three major flotation classes: raft-like profiles that include proteins peaking at either of the light fractions (f) 3–6 (clusters P1-P3), complex buoyancy profiles (cluster 4), and profiles that include proteins floating in heavy fractions 7 and/or 8 (clusters P5-P6); (**B**) The distribution of flotation classes in the DRM proteomes is shown as pie charts. (**C**) DRM proteomes of early and late schizonts, and gametocytes are organized by functional categories and the percentages of proteins falling in the three flotation classes are shown as bars. The number of proteins in each category is indicated in the horizontal axis.

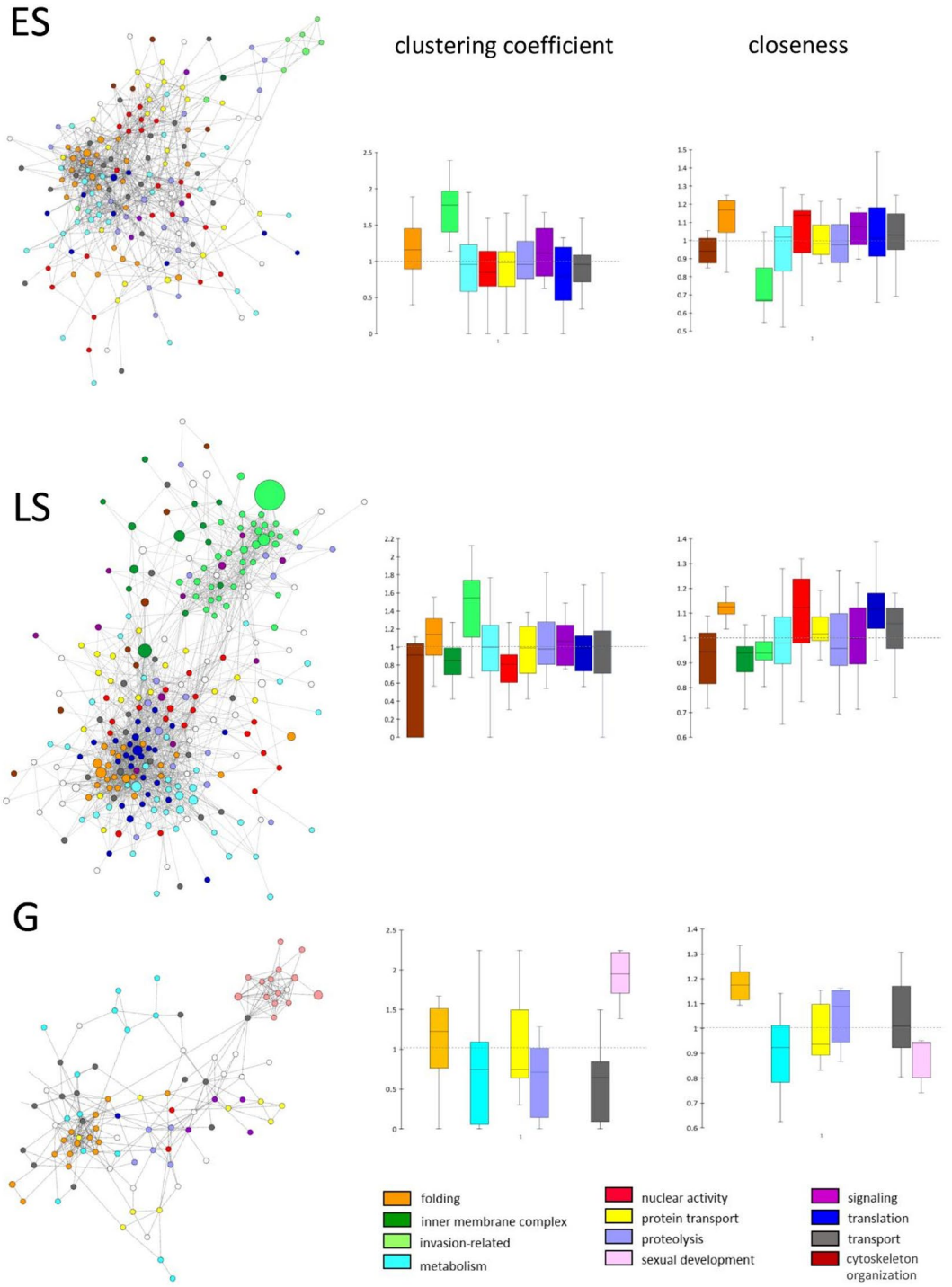

Fig. 3. Protein-protein interaction (PPI) networks of stage-related DRM proteomes. Global protein-protein interaction network inferred for *P. falciparum* was filtered by DRM-associated proteins of early schizonts (ES), late schizonts (LS) and gametocytes (G) to obtain stage-related DRM interactomes. Dots represent proteins and are colored according to their functional annotations; node size is proportional to estimated total abundance. Measures of centrality (clustering coefficient and closeness) were estimated and normalized (dashed line; mean value equal 1) for all proteins in the functional categories and the corresponding distributions reported as box plots.

Host junctional complex components are mobilized and recruited to parasite DRMs

DRM proteomes of asexual and sexual blood stages include a total of 29 host proteins (Table S6) also identified in DRMs of healthy erythrocytes[29] with the exclusion of Methanethiol oxidase. This subset of proteins accounts for about 20% of the host DRM proteome[29] and includes proteins involved in cell redox homeostasis, transport,

Category	T_D-ES_D-LS_D	T-ES_D-LS_D	T-ES_D	T-LS_D	LS_D	*N°* of proteins
Cell redox homeostasis	42.9	14.3	14.3	28.6	0.0	7
Folding	27.3	24.2	30.3	18.2	0.0	33
Inner membrane complex	7.7	7.7	0.0	84.6	0.0	13
Invasion-related	22.9	2.9	2.9	48.6	22.9	35
Metabolism	33.3	26.2	7.1	31.0	2.4	42
Nuclear activity	3.8	53.8	23.1	19.2	0.0	26
Protein transport	39.1	34.8	17.4	8.7	0.0	23
Proteolysis	25.0	35.0	25.0	10.0	5.0	20
Signaling	7.1	21.4	7.1	50.0	14.3	14
Translation	7.7	23.1	7.7	57.7	3.8	26
Transport	23.1	46.2	23.1	7.7	0.0	26
Catabolism	0.0	50.0	16.7	33.3	0.0	6
Cytoskeleton organization	0.0	71.4	0.0	28.6	0.0	7
Erythrocyte remodeling	0.0	33.3	0.0	66.7	0.0	6
Endocytosis	0.0	0.0	0.0	100.0	0.0	5

Table 1. Dynamics of protein recruitment in DRMs during asexual parasite development. Percentage of proteins in different functional categories detected in DRMs of trophozoites (T_D), early schizonts (ES_D) and late schizonts (LS_D) or in global proteome of trophozoites (T) but recruited in DRMs of early and/or late schizonts; 22,9% and 14,3% of proteins involved in invasion and signal transduction, respectively, reside exclusively in DRMs of late schizonts.

Category	Conserved	Cariable	No of proteins
Cell redox homeostasis	25.0	75.0	4
Folding	76.5	23.5	17
Invasion-related	66.7	33.3	9
Metabolism	67.9	32.1	28
Nuclear activity	26.7	73.3	15
Protein transport	76.5	23.5	17
Proteolysis	75.0	25.0	12
Signaling	75.0	25.0	4
Translation	37.5	62.5	8
Transport	35.0	65.0	20
Cytoskeleton organization	40.0	60.0	5

Table 2. Comparative analysis of the flotation properties of DRM proteins detected in early and late schizonts. Percentages of proteins common to early and late schizonts with conserved/variable flotation profiles in different functional categories.

and proteins with a role in raft organization. In addition, about half of the host proteins copurified with the parasite DRMs participate to the supramolecular junctional complex with an essential role in forming bridges between the actin-spectrin skeleton and membrane proteins. Among the latter, we identified Glucose transporter member 1 (Glut 1), Band3, Glycophorin-A, Kell blood group, while the skeletal adaptor molecules detected are: the actin-binding proteins 4.1, α/β-Adducins, Protein 4.2 and 55 kDa erythrocyte membrane protein (P55) (see also Table S6). Interestingly, the flotation profiles of the host DRM proteins identified in this study largely differ from those observed in healthy erythrocytes (Table S6 and Figure S3). These observations support a DRM-mediated reorganization of structural components of RBCs during *Plasmodium* infection. To verify this, we decided to investigate the subcellular compartmentalization of the skeletal adaptor protein β-*addu*cin during infection, using biochemical and immunolocalization approaches. As shown in Fig. 4A, β-adducin is recruited by the parasite and maintained during asexual and sexual development of blood stages.

To confirm the inclusion of β-adducin in subcellular compartments of parasite origin, we separated intact parasites surrounded by PVM from host RBC ghosts by selective permeabilization of the RBC membrane with Streptolysin-O. Vacuolar parasites were treated with Triton-X100 and soluble and insoluble fractions prepared. In Western blot analysis (Fig. 4B) antibodies specific for β-adducin detected this skeletal protein in ghost and in Triton-insoluble parasite fraction.

To define the topology of internalized β-adducin, we treated vacuolar parasites and ghosts of infected and non-infected RBCs with Proteinase K and probed them with antibodies specific for β-adducin (Fig. 4C). In the infected and non-infected RBC ghosts, β-adducin was sensitive to PK digestion, whereas in the vacuolar

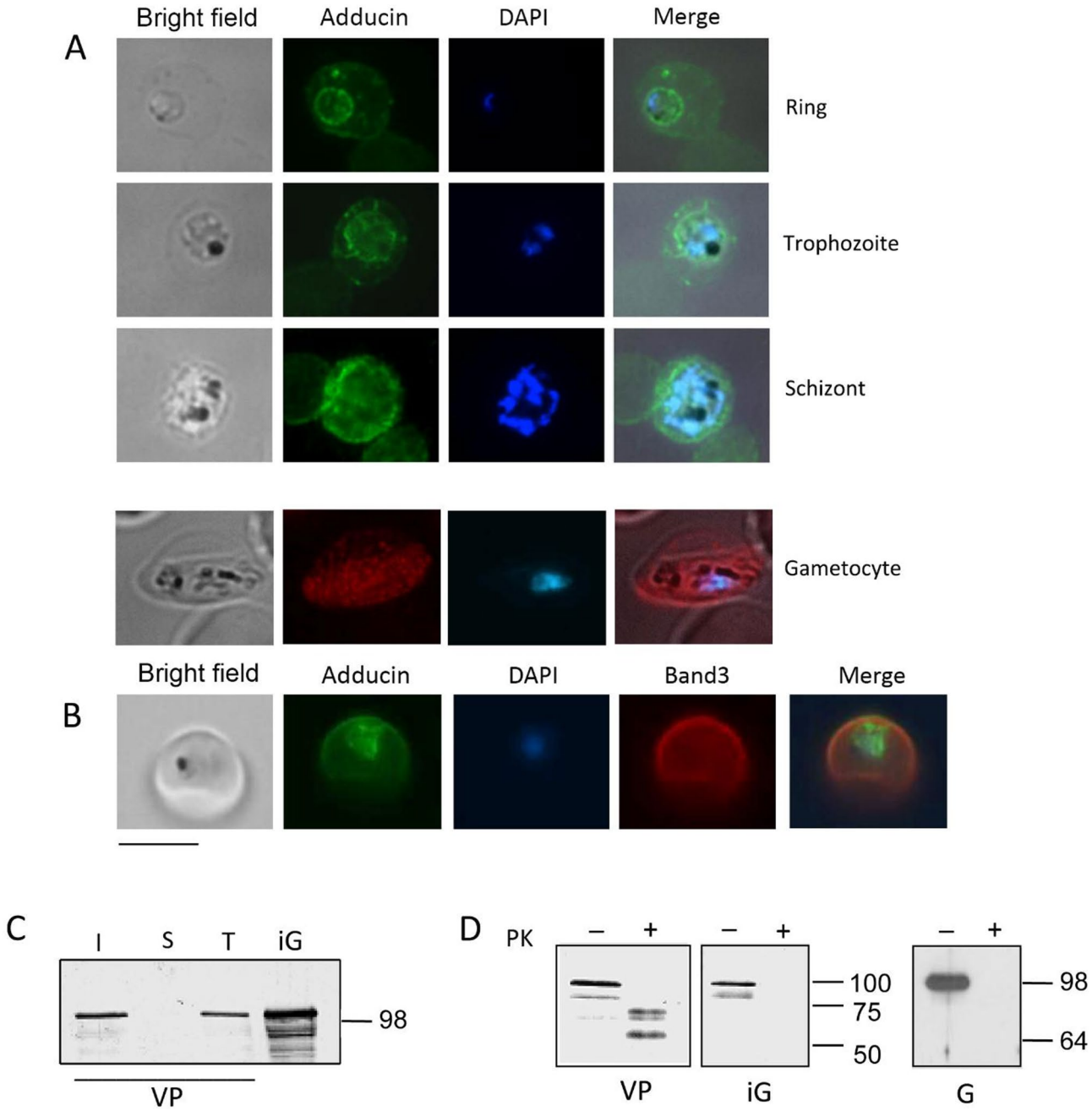

Fig. 4. Subcellular localization and topology of β-adducin in *P. falciparum* iRBCs. (**A**) immuno localization of β-adducin shows internalization of this host protein during blood stage parasite development. (**B**) double IFA using antibodies against β-adducin and Band3 indicates that this latter is not recruited by the parasite. Nuclei were stained with DAPI. Scale bar 5 µm. (**C**) Vacuolar parasites (VP) and ghosts, prepared from SLO-treated iRBCs (iG), were incubated with Triton-X100. Triton-insoluble (I) and soluble (S) parasite fractions, and unfractionated parasite (T) were probed with antibodies against β-adducin. (**D**) Ghosts from iRBC (iG), RBC (G) and purified vacuolar parasites (VP), obtained after SLO treatment, were incubated with or without Protease K (PK) and analyzed by western blot using anti-β-adducin antibodies.

parasites β-adducin was partially protected, as indicated by multiple bands of lower molecular size compared with the single band corresponding to the intact protein detected in the control sample (Fig. 4D). These results suggest that β-adducin localizes to the periphery of the PV and is partially exposed to PK degradation. Notably, the N-terminus of the protein should face the host cell cytosol since the immune serum used was raised against the C-terminus.

Using specific antibodies in IFA experiments on iRBCs (Figure S3), we showed that P55, a second adaptor molecule, colocalizes with the DRM-associated RBC protein ART4, ADP-ribosyltransferase 4, which is recruited

in the parasite PVM upon infection[29]. We also confirmed that the integral membrane proteins Band3 (Fig. 4C), anchored to the underlying skeleton, is not internalized, as shown in previous studies[30].

Discussion

In this study, we analyzed the dynamics of membrane microdomains during *P. falciparum* schizont maturation and compared their organization with that of stage IV/V gametocytes. We isolated these membrane assemblies as detergent-resistant membranes (DRMs) by sucrose gradient centrifugation, taking advantage of their peculiar resistance to solubilization in cold non-ionic detergents. We identified 216 proteins in early schizonts, 292 in late schizonts and 121 in mature gametocytes. Previous studies on the DRM proteomes of *P. falciparum* trophozoites[3] and *P. beghei* gametocytes[21] show an overlap of 94% and 92%, respectively, with the DRM proteomes analyzed in this study.

We defined the composition and abundance of proteins and fatty acids in each gradient fraction, by quantitative mass spectrometry and gas chromatography analysis, and constructed for each identified protein an abundance profile (PAP) along the gradient that relates to the flotation properties of DRMs[21,29]. The entire repertoire of PAPs in DRM proteomes of schizonts (early and late) and mature gametocytes was subjected to unsupervised cluster analysis to define major flotation profiles. We, then, classified as raft-like DRMs, those assemblies with protein components peaking in light gradient fractions 3–6, and heavy DRMs those with proteins floating in fraction 7 and 8, closer to the loading zone at the bottom of the gradient.

Consistently, we found an abundance of saturated fatty acids in light fractions 3–6, characteristic of tightly packed, liquid ordered membrane organization[31] that are resistant to solubilization, while a higher content of mono- and poly-unsatured fatty acids in the heavy fractions 7 and 8, probably responsible for the formation of less-ordered microdomains, more prone to solubilization. Interestingly, we also observed more complex profiles that likely include proteins recruited in multiple DRMs with different structural organization.

The construction of protein and fatty acid profiles along the gradient provided a tool to compare the composition, structural organization, and dynamics of DRMs in different blood stages of *Plasmodium*.

The DRM proteomes of asexual schizonts (early and late), committed to produce invasive merozoites, and sexual gametocytes, precursors of gametes, share a core of 70 proteins involved mainly in metabolic processes, protein trafficking and nuclear activities. However, only 38.6% of them exhibit the same buoyancy characteristics between stages, suggesting that most of these proteins are embedded in different membrane contexts.

We analyzed in more detail two common proteins, the thioredoxin-like protein (PF3D7_1104400), involved in RBC invasion, and localized in the apical portion of merozoites and in the PVM of trophozoites[15] and the PV-resident P113 (PF3D7_1420700)[16] a component of the parasite export complexes PTEX[17] and EPIC[18]. In contrast to asexual stages, in which both proteins reside in the PV compartment, in mature gametocytes they are exported in vesicle-like structures to the cytosol and periphery of the RBC, suggesting new interactions and functions for them that are specific to the sexual stage.

Based on the architecture of the protein-protein interaction networks predicted for the three stage-related DRM proteomes, the common core proteins form a highly interconnected central subnetwork, while stage-specific functions form peripheral clusters, poorly connected with the rest of the network.

The majority of the stage-specific proteins involved in host cell invasion have been identified only in DRMs of late schizonts, where they reside in raft-like microdomains. These include merozoite proteins of specialized secretory compartments, the rhoptry bulb/neck and micronemes, as well as components of the merozoite plasma membrane and the underlying inner membrane complex.

Comparative analysis of the DRM proteomes of trophozoites[3] early and late schizonts (this study) with that of the global proteome of trophozoite (PlasmoDB) showed that 80% of the components of the inner membrane complex/gliding motility and about 50% of the invasion-related proteins are expressed at the trophozoite stage but recruited into microdomains only in late schizonts. This indicates that protein recruitment in cholesterol-rich membrane microdomains is not necessarily coupled to protein expression, and may serve to spatially and temporally regulate the execution of biological processes.

In the case of gametocytes, some proteins that reside in DRMs are specifically involved in processes that occur in the mosquito midgut, when gametogenesis is triggered. These include LCCL-domain containing proteins that form multiprotein complexes contributing to the adhesiveness of the emerging gametes[32]. We also identified the putative secreted ookinete proteins PSOP1[33] and PSOP12[34], and the ookinete surface proteins P25[35] abundantly expressed on the ookinete surface with an important role in parasite recognition and attachment to the mosquito midgut.

Plasmodium parasite extensively remodels the host erythrocyte upon invasion by generating membranous structures (MCs and PVM), which contain cholesterol-rich microdomains[3], involved in translocating parasite proteins to the cytosol, skeleton, and membrane of the host RBC, thereby linking the host and parasite compartments. We identified a member (PF3D7_0936800) of the PHIST (Plasmodium helical interspersed subtelomeric) family in the DRM proteome of late schizonts and a second member PF3D7_1102500, also known as PfGEXP02, in the DRMs of gametocytes. It has been reported that PF3D7_0936800 is translocated to the membrane of iRBC in asexual stages[36] while PF3D7_1102500 interacts with the cytoskeleton of iRBCs[20].

Infection of erythrocytes by malaria parasite also results in the selective recruitment of host proteins residing in erythrocyte membrane microdomains and their relocation in parasite-specific structures[30]. These include the signaling GTPases Gαs[37] and Rac1[38]; the raft organizer proteins Flotillin1 and 2, the beta-2 adrenergic receptor (β2-AR), the Duffy blood group, and the erythrocyte antigens CD55, CD58, CD59[37]; the membrane water channel Aquaporin-1 (AQP1), and the ADP-ribosyltransferase 4 (Art 4)[29]. Other abundant erythrocyte membrane proteins, such as Band3, Glut1 or Stomatin are excluded[37].

In this study we showed that the DRM proteomes of asexual and sexual blood stages of *P. falciparum* collectively comprise 28 host proteins, accounting for 20% of the DRM proteome of healthy RBCs[29]. Notably, sixteen of

these proteins are components of the junctional complex, which connects the RBC membrane to the underlying actin-spectrin cytoskeleton via adaptor molecules[39]. Immunolocalization and biochemical approaches indicated that the adaptor molecule β adducin and p55 are mobilized and internalized by the invading parasite becoming component of the nascent PVM. Furthermore, in a previous study[40]we demonstrated that the adaptor molecule dematin is also recruited into parasite compartments of the in both *P. falciparum* and *P. berghei* iRBCs.

Interestingly, we also observed that the buoyancy properties of the internalized proteins differ largely from those observed in healthy RBCs[29]confirming that they are moved to different membrane contexts.

These observations suggest that the coordinated remodeling of the host erythrocyte upon invasion, is likely mediated by cholesterol-rich membrane microdomains, which are exploited and largely reorganized by the parasite.

Materials and methods

Ethics approval

Blood was obtained from the Transfusion Center of Policlinico Umberto I for analyzing erythrocyte proteins and propagate *P. falciparum* cultures. The experimental protocol was approved by the "Policlinico Umberto I Ethics Committee". All methods were performed by relevant guidelines and regulations on the suitability assessment of blood donors and blood components (Ministry of Health-Decree of 3 March 2005, Official Gazette no 85, 13-4-2005). Blood samples were screened for known pathogens by the Italian National Regulations.

Statement on informed consent obtained from the participants

No information about the donor, other than the blood group was obtained or recorded by the user. Written informed consent was obtained from blood donors and collected by the hospital personnel, including a statement that participation was voluntary. No minors were included in this study.

Parasite culture, synchronization, and purification

According to standard methods[41] *P. falciparum* 3D7 line was maintained in culture in human 0 + erythrocytes.

Parasites were tightly synchronized by isolating schizonts on a 60% Percoll gradient[42] followed by a 4-hour reinvasion period in fresh erythrocytes. Residual schizonts were subsequently eliminated by sorbitol treatment[43] yielding a population of parasites with a defined 4-hour age window. Schizonts were then isolated at two time points: 36- and 46-hours post-invasion (hpi), by using the MACS® column-based magnetic separation system[44].

To isolate sexual stages, parasites were induced to undergo gametocytogenesis by nutrient starvation. Asexual stages were subsequently cleared 24 h post-induction by treatment with 0.05 M N-acetylglucosamine, resulting in a synchronous gametocyte population[45]. On day 9 post-induction, stage IV/V *P. falciparum* gametocytes were purified using a 60% Percoll gradient to remove uninfected erythrocytes[46].

DRMs Preparation

iRBCs were centrifuged (900 × g, 10 min) and RBC membranes selectively ruptured by resuspending cell pellet in 20 volumes of cold lysis buffer (0.15 M NH4Cl, 0.01 M KHCO3, 1 mM EDTA) in the presence of protease inhibitors (Roche). This osmotic lysis disrupts the erythrocyte membrane, maintaining intact parasites surrounded by the PVM[47]. After 10–15 min in ice, free vacuolar parasites were collected by centrifugation and washed three times in PBS to remove hemoglobin.

To isolate DRMs, 3×10^8 vacuolar parasites were suspended in 0.75 ml of MES-buffered saline (25 mM MES, pH 6.5, 0.15 M NaCl) containing 1% Triton X-100 (v/v) and homogenized with a potter-elvehjem glass homogenizer. Cell extracts were adjusted to 40% sucrose by the addition of 0.75 ml of 80% sucrose in MES-buffered saline, placed at the bottom of an ultracentrifuge tube (4.5 ml, 13 × 15 mm, Beckman) and overlaid with 1.5 ml of 30% and 1.5 ml of 5% sucrose. Samples were subjected to equilibrium density gradient centrifugation using SW60Ti rotor (Beckman) at 45,000 rpm (208,000 × g), for 18 h at 4 °C. 375-µl fractions were then collected from the top of the gradient. Under our conditions, DRMs float in the lighter fractions 2–8, while detergent-soluble membranes (DSM) remain in the loading zone (fractions 9–12). Sucrose density of the collected fractions was routinely determined through refractive index values to check the linearity of the gradient. The effectiveness and reproducibility of gradient fractionation were always verified by probing DRM containing fractions 2–8 with antibodies specific for Flotillin 1, a well-characterized raft marker of red blood cells. Under our working conditions, Flotillin 1 floats to light fractions 4–5, as shown in previous studies[21,29]. Proteins in light fractions 2–8 were precipitated, as described[21]whereas lipids were extracted as described[48].

Subcellular fractionation of iRBC

To prepare total Triton-insoluble and -soluble parasite extracts, 10^7cell were spun and resuspended in 0.1 ml of cold MES-buffered saline supplemented with 1% Triton X-100, homogenized as described above, and centrifuged 30 min at 30,000 × g. Soluble fractions were collected, while the pellets were washed in cold MES-buffered saline. Insoluble fractions were recovered after centrifugation (30 min at 30,000 × g) and resuspended in 0.1 ml volume of SDS-PAGE loading sample buffer.

Proteinase K digestion assay

Purified *P. falciparum* iRBCs were incubated 30 min at 37 °C with Streptolysine-O (SLO) (La Technique Biologique, Paris, France) to permeabilize the RBC membrane, leaving intact the PVM. iRBC cytoplasm and parasites were separated by low-speed centrifugation (2000 g x 10 min at 4 °C). iRBC cytoplasm was successively spun down at high speed (15000 g x 30 min at 4 °C) to recover ghosts. Parasite pellet and ghosts were extensively washed with PBS. Proteinase K (Roche Diagnostics GmbH, Mannheim, Germany) treatment was performed on

purified vacuolar parasites and iRBC ghosts as described[49]. Samples were separated by SDS-PAGE and analyzed by Western blot.

Antibodies

anti-P55 (SantaCruz) mouse monoclonal 1:1000 in WB, 1:100 in IFA, anti-GAPDH rabbit polyclonal 1:1000 in WB (SantaCruz). anti-β-adducin rabbit polyclonal against the amino acids 581–700 of β-adducin C-terminus 1:1000; IFA 1:30 (H-120, Santa Cruz).

Western blot analysis

Uninfected RBCs samples were obtained from blood of 7 healthy donors. Briefly, RBCs were washed 3 times in RPMI (Gibco) to remove all serum, platelets, and white blood cells. Infected RBCs were prepared as previously described for DRM purification. Both healthy and iRBCs were counted with a Buerker hemocitometer. 2×10^6 healthy and 2×10^6 iRBCs were lysed in 2x Laemmli Sample Buffer and subjected to SDS-Page under reducing conditions, followed by transfer on nitrocellulose membrane (ThermoFisher). The filters were hybridized with primary antibodies and then with anti-mouse or anti-rabbit HPR-conjugated secondary antibodies 1:10000 (Pierce). Immunocomplexes were visualized using a chemioluminescence detection system (ThermoFisher) with a ChemiDOC Imagin System (BioRad).

Indirect Immunofluorescence assay (IFA)

Blood smears were fixed on glass slides for 1 h with 4% paraformaldehyde at room temperature (RT), washed in PBS, treated with 0.1% Triton X-100 in PBS (10 min at RT) and washed again in PBS. Blocking was performed 1 h in PBS/3% BSA at RT. Slides were then incubated 1 h in primary antibody, washed in PBS, and incubated 30 min in fluorescein- or rhodamine-conjugated goat α-mouse or α-rabbit secondary antibodies (1:400 dilution). Cell nuclei were labeled with 4′,6-diamidin-2-fenilindolo (DAPI). The specificity of the immune sera was checked in parallel using pre-immune sera.

Mass spectrometry analysis

Protein contents from the sucrose gradient fractions 2–8 were loaded on SDS-PAGE (home-made 5% stacking-12% resolving bis-tris-PAGE) and run just to allow the Protein Marker (BenchMark™ Pre-Stained Protein Ladder, Invitrogen) to enter the resolving gel. After Coomassie Staining (Novex, Colloidal Blue Staining gel, Invitrogen) unresolved bands were excised and in-gel tryptic digestion was performed as already described [ref].Briefly, gel slices were destained by washings in acetonitrile (ACN)/50 mM NH4CO3 (1:1), treated with 10 mM DTT (40 min at 56 °C) and 55 mM iodoacetamide (30 min in the dark at RT) to reduce and alkylate cysteines, shrunken with ACN and rehydrated for 40 min on ice with a solution of 12,5 ng/µl trypsin (Promega) in 50 mM NH4CO3. Then, the trypsin solution was replaced with 25 mM NH4CO3, and protein digestion was carried out overnight at 37 °C. Supernatants were dried in speedvac, resuspended in 20 µL of HPLC buffer A (95% ACN, 0.1% FA) and used for LC-MS/MS analysis.

Nano-RPLC was performed using a nano-HPLC 3000 Ultimate (Dionex) connected on line to LTQ-XL linear ion trap (Thermo Fisher). Tryptic digests were firstly loaded on a C18 RP-precolumn (300 µm i.d.x5 mm; 5 µm particle size; 100 Å pore size; LC Packings-Dionex), washed by the loading pump at 20µL/min with buffer A for 5 min and then on an homemade 13 cm x 75 µm- i.d. Silica PicoTip (8 ± 1 µm) column (PicoTip Emitter, NewObjective) packed with Magic C18AQ (5 µm particle size; 200 Å pore size, Michrom Bioresouces Inc.) for chromatographic separations. Peptides were eluted at 0.3 µL/min along a 120 min linear gradient from 15 to 60% of buffer B (95% ACN, 0.1% FA) and electrosprayed directly into the mass spectrometer with a spray voltage of 1.60–1.65 kV and a capillary temperature of 180 °C. Data acquisition was performed in data-dependent Top5. Full-scan MS parameters settings were: automatic gain control value of 30,000 ions; maximum injection time of 10 ms; m/z 400–2000 mass range. The five most intense ions were sequentially selected and fragmented in CID mode with the following parameters settings: isolation width of 2.0; automatic gain control value of 10,000 ions; maximum injection time of 100 ms; m/z 50-2000 mass range; collision energy of 35%; minimum signal threshold of 100 counts, wide band activation was on. A dynamic exclusion of ions previously sequenced within 60 s was applied.

Spectra files were analyzed by Sequest search engine with Proteome Discoverer 1.4 (ThermoFisher) using a homemade database constructed with the Human Uniprot-Swissprot database (released on August 2020) and Pfalciparum3D7__48 (released on August 2020 on Plasmodb) and containing also decoy database. The Carboamidomethylation of cysteines was specified as fixed modification and the oxidation of methionine was set as variable modification; mass tolerance was set to 0.8 Da for-precursor ion and 0.4 Da for-fragment ions and a maximum of two missed cleavages was allowed. The Percolator tool was used for peptide validation based on the q-value and high confidence was chosen, corresponding to a false discovery rate (FDR) ≤ 1% on the peptide-level. Proteins were identified with a minimum of 2 peptides rank = 1. Proteins purified from each developmental stage were identified by liquid chromatography-tandem mass spectrometry (LC-MS/MS) in three biological replicates.

Lipid analysis

Lipids were extracted from gradient fractions 3–8 using a chloroform/methanol (2:1, v/v) solution according to the procedure described by Folch[48]dried under nitrogen atmosphere and used for neutral lipid and phospholipid HPTLC. HPTLC for neutral lipids was done by eluting lipid extract in a hexane/diethylether/acetic acid (70:30:1, v/v). HPTLC for phospholipids was performed by running lipid extract in a chloroform/methanol/acetic acid/formic acid/H2O (35:15:6: 2:1, v/v), to separate SM, PC, and PE. The spots were visualized via copper acid staining (3% w/v). The plate was heated for about 5 min at 180 °C, and the abundance of the different lipid classes

in each fraction was estimated in comparison with lipid standards (Sigma-Aldrich Corporation, St. Louis, MO) using a GS-700 imaging densitometer (Bio-Rad).

The fatty acid-containing glycerophospholipids of the DRM fractions were transformed into the corresponding fatty acid methyl esters (FAMEs) after treatment of the phospholipid extracts with 0.5 M KOH in methanol (0.5 mL), stirred for 10 min at room temperature under an inert atmosphere, and quenched with 0.5 mL of brine. FAMEs were extracted with *n*-hexane (3 × 2 mL), and the combined organic phases were dried over anhydrous Na_2SO_4 and evaporated to dryness. The FAME residues were dissolved in 10 µL of *n*-hexane, and 1 µL was injected into the GC for analysis. The applied mild transesterification conditions ensured quantitative polyunsaturated fatty acid (PUFA) recovery in the DRM phospholipid fractions[50]. The fatty acid composition was expressed as relative percentages of the quantitative FAME values obtained from two replicates.

Fatty acid methyl esters (FAME) were analyzed by gas chromatography (GC) using an Agilent 6850 instrument (Agilent, Cernusco sul Naviglio, Milan, Italy) equipped with a 60 m × 0.25 mm × 0.25 µm DB23 column (Agilent, Milan, Italy) and operated in split mode (50:1). FAMEs were identified by comparison with authentic standards and quantified using calibration curves, following established protocols[50–52]. *Cis* and commercially available *trans*-FAME standards were purchased from Merck (Darmstadt, Germany), and 6*cis*-hexadecenoic acid methyl ester was purchased from Lipidox (Lidingö, Sweden). All solvents (HPLC grade) such as *n*-hexane, methanol, and reagents, potassium hydroxide (KOH), anhydrous sodium sulfate (Na_2SO_4) were purchased from Carlo Erba (Cornaredo, Milan, Italy) and used without further purification.

The efficiency of the extraction-transesterification procedures was estimated at 90 ± 3% based on the theoretical yield expected from the starting PL and using an internal calibration standard (C17:0). Quantitative analysis was performed using the calibration factors of each FAME. The relative abundance of fatty acids in each gradient fraction was expressed as mean percentage values of two replicates.

Statistical analysis

Quantitative proteomics and fatty acid analysis were applied to characterize buoyancy profiles of identified proteins (three biological replicates) and lipids (two biological replicates) in fractions 2–8. Protein abundances of the three biological replicates were determined by label-free quantification (LFQ)[53]. Common proteins were used to derive a normalization coefficient, calculated as the ratio of the total abundance of a fraction to the abundance of the same fraction of the replicate with the highest total abundance. The reproducibility of the normalized LFQ values was preliminarily assessed with an ANOVA test (95% confidence interval; tolerance 10 − 4). We then constructed the abundance profile along the gradient of each protein detected (PAP)[21]. The reproducibility of the PAPs was assessed by correlation analysis (details in additional data). All statistical analyses were conducted by XLSTAT- Lumivero (2024). XLSTAT statistical and data analysis solution [https://www.xlstat.com/en]. Once the robustness of PAPs was verified, LFQ values of proteins identified in more than one replicate were averaged to obtain a single profile per protein. For comparative purposes, we generated reference PAPs representative of buoyancy characteristics of the three stage-related DRM proteomes. To this end, we submitted the entire PAP repertoire of the three stages to a K-mean cluster analysis (similarity metric = Pearsons correlation coefficient) by Gene Cluster 3.0[54]. The optimal number of 6 clusters was determined by Elbow method in Rstudio 2022.02.3.

We inferred a global protein-protein interaction (PPI) network for *P. falciparum* using a Bayesian approach. The network includes information on gene-expression information of asexual and sexual stages. We also constructed new genomic datasets (rosetta-stone and phylogenetic profiles) to improve the robusteness and predictive performance of the interactome[23] (details in Additional data).

Data from the different sources were integrated as described in Additional data to derive a score (LG) for each protein pair, indicating the reliability of that interaction. An assessment procedure was conducted by comparing protein-protein interactions with gold standard datasets based on the KEGG metabolic pathway database. A threshold score (LG ≥ 7) was established to ensure a true positive (TP)/false positive (FP) ratio ≥ 10 and a genome coverage > 90%. This resulted in a protein-protein interaction network of 4805 proteins and 403,239 edges. The DRM proteomes of early and late schizonts and gametocytes were then used to filter the global PPI network and derive the corresponding interactomes. The PPI networks were visualized and analyzed with CytoScape3.10.1[55].

Data availability

Spectra raw files and database are available on Massive Repository: Dataset MSV000097440 (ProteomeXchange dataset PXD062207) [ftp://massive-ftp.ucsd.edu/v09/MSV000097440](ftp:/massive-ftp.ucsd.edu/v09/MSV000097440) . Username for web access: MSV000097440_reviewer; Password: R@ftF@lc.

Received: 20 June 2025; Accepted: 28 August 2025
Published online: 03 October 2025

References

1. Farrow, R. E. et al. The mechanism of erythrocyte invasion by the malarial parasite, plasmodium falciparum. *Semin Cell. Dev. Biol.* **22**, 953–960. https://doi.org/10.1016/j.semcdb.2011.09.022 (2011).
2. Groomes, P. V., Kanjee, U. & Duraisingh, M. T. RBC membrane biomechanics and plasmodium falciparum invasion: probing beyond ligand-receptor interactions. *Trends Parasitol.* **38**, 302–315. https://doi.org/10.1016/j.pt.2021.12.005 (2022).
3. Yam, X. Y. et al. Proteomic analysis of detergent-resistant membrane microdomains in trophozoite blood stage of the human malaria parasite plasmodium falciparum. *Mol. Cell. Proteom.* **12**, 3948–3961. https://doi.org/10.1074/mcp.M113.029272 (2013).
4. Koudatsu, S. et al. Glycosphingolipid GM3 is localized in both Exoplasmic and cytoplasmic leaflets of plasmodium falciparum malaria parasite plasma membrane. *Sci. Rep.* **11**, 14890. https://doi.org/10.1038/s41598-021-94037-3 (2021).
5. Sanders, P. R. et al. Distinct protein classes including novel merozoite surface antigens in Raft-like membranes of plasmodium falciparum. *J. Biol. Chem.* **280**, 40169–40176. https://doi.org/10.1074/jbc.M509631200 (2005).
6. Simons, K. & Ikonen, E. Functional rafts in cell membranes. *Nature* **387**, 569–572. https://doi.org/10.1038/42408 (1997).

7. Brown, D. A. Analysis of raft affinity of membrane proteins by detergent-insolubility. *Methods Mol. Biol.* **398**, 9–20. https://doi.org/10.1007/978-1-59745-513-8_2 (2007).
8. Lingwood, D. & Simons, K. Lipid rafts as a membrane-organizing principle. *Science* **327**, 46–50. https://doi.org/10.1126/science.1174621 (2010).
9. Sezgin, E., Levental, I., Mayor, S. & Eggeling, C. The mystery of membrane organization: composition, regulation and roles of lipid rafts. *Nat. Rev. Mol. Cell. Biol.* **18**, 361–374. https://doi.org/10.1038/nrm.2017.16 (2017).
10. Samuel, B. U. et al. The role of cholesterol and glycosylphosphatidylinositol-anchored proteins of erythrocyte rafts in regulating raft protein content and malarial infection. *J. Biol. Chem.* **276**, 29319–29329 (2001).
11. Koshino, I. & Takakuwa, Y. Disruption of lipid rafts by Lidocaine inhibits erythrocyte invasion by plasmodium falciparum. *Exp. Parasitol.* **123**, 381–383 (2009).
12. Maier, A. G. & van Ooij, C. The role of cholesterol in invasion and growth of malaria parasites. *Front. Cell. Infect. Microbiol.* **12**, 984049. https://doi.org/10.3389/fcimb.2022.984049 (2022).
13. Hayakawa, E. H., Yamaguchi, K., Mori, M. & Nardone, G. Real-time cholesterol sorting in plasmodium falciparum-erythrocytes as revealed by 3D label-free imaging. *Sci. Rep.* **10**, 2794. https://doi.org/10.1038/s41598-020-59552-9 (2020).
14. Siau, A. et al. Comparative Spatial proteomics of Plasmodium-infected erythrocytes. *Cell. Rep.* **42**, 113419. https://doi.org/10.1016/j.celrep.2023.113419 (2023).
15. Wang, W. et al. A thioredoxin homologous protein of plasmodium falciparum participates in erythrocyte invasion. *Infect. Immun.* **86** https://doi.org/10.1128/IAI.00289-18 (2018).
16. Bullen, H. E. et al. The plasmodium falciparum parasitophorous vacuole protein P113 interacts with the parasite protein export machinery and maintains normal vacuole architecture. *Mol. Microbiol.* **117**, 1245–1262. https://doi.org/10.1111/mmi.14904 (2022).
17. de Koning-Ward, T. F. et al. A newly discovered protein export machine in malaria parasites. *Nature* **459**, 945–949. https://doi.org/10.1038/nature08104 (2009).
18. Hakamada, K. et al. PV1 protein from plasmodium falciparum exhibits chaperone-Like functions and cooperates with Hsp100s. *Int. J. Mol. Sci.* **21** https://doi.org/10.3390/ijms21228616 (2020).
19. Sargeant, T. et al. (ed, J.) Lineage-specific expansion of proteins exported to erythrocytes in malaria parasites. *Genome Biol.* **7** R12 https://doi.org/10.1186/gb-2006-7-2-r12 (2006).
20. Warncke, J. D. et al. The PHIST protein GEXP02 targets the host cytoskeleton during sexual development of plasmodium falciparum. *Cell. Microbiol.* **22**, e13123. https://doi.org/10.1111/cmi.13123 (2020).
21. Fratini, F. et al. An integrated approach to explore composition and dynamics of Cholesterol-rich membrane microdomains in sexual stages of malaria parasite. *Mol. Cell. Proteom.* **16**, 1801–1814. https://doi.org/10.1074/mcp.M117.067041 (2017).
22. Jansen, R. et al. A bayesian networks approach for predicting protein-protein interactions from genomic data. *Science* **302**, 449–453. https://doi.org/10.1126/science.1087361 (2003).
23. Sferra, G., Fratini, F., Ponzi, M. & Pizzi, E. Phylo_dCor: distance correlation as a novel metric for phylogenetic profiling. *BMC Bioinform.* **18**, 396. https://doi.org/10.1186/s12859-017-1815-5 (2017).
24. Le Roch, K. G. et al. Discovery of gene function by expression profiling of the malaria parasite life cycle. *Science* **301**, 1503–1508. https://doi.org/10.1126/science.1087025 (2003).
25. Young, J. A. et al. The plasmodium falciparum sexual development transcriptome: a microarray analysis using ontology-based pattern identification. *Mol. Biochem. Parasitol.* **143**, 67–79. https://doi.org/10.1016/j.molbiopara.2005.05.007 (2005).
26. Date, S. V. & Stoeckert, C. J. Computational modeling of the plasmodium falciparum interactome reveals protein function on a genome-wide scale. *Genome Res.* **16**, 542–549. https://doi.org/10.1101/gr.4573206 (2006).
27. Goenawan, I. H., Bryan, K. & Lynn, D. J. DyNet: visualization and analysis of dynamic molecular interaction networks. *Bioinformatics* **32**, 2713–2715. https://doi.org/10.1093/bioinformatics/btw187 (2016).
28. Silvestrini, F. et al. Protein export marks the early phase of gametocytogenesis of the human malaria parasite plasmodium falciparum. *Mol. Cell. Proteom.* **9**, 1437–1448. https://doi.org/10.1074/mcp.M900479-MCP200 (2010).
29. Olivieri, A. et al. Structural organization of erythrocyte membrane microdomains and their relation with malaria susceptibility. *Commun. Biol.* **4**, 1375. https://doi.org/10.1038/s42003-021-02900-w (2021).
30. Murphy, S. C. et al. Lipid rafts and malaria parasite infection of erythrocytes. *Mol. Membr. Biol.* **23**, 81–88. https://doi.org/10.1080/09687860500473440 (2006).
31. Kinnun, J. J., Bolmatov, D., Lavrentovich, M. O. & Katsaras, J. Lateral heterogeneity and domain formation in cellular membranes. *Chem. Phys. Lipids*. **232**, 104976. https://doi.org/10.1016/j.chemphyslip.2020.104976 (2020).
32. Bennink, S. & Pradel, G. The multiple roles of LCCL Domain-Containing proteins for malaria parasite transmission. *Microorganisms* **12** https://doi.org/10.3390/microorganisms12020279 (2024).
33. Tachibana, M., Iriko, H., Baba, M., Torii, M. & Ishino, T. PSOP1, putative secreted Ookinete protein 1, is localized to the micronemes of plasmodium yoelii and P. berghei Ookinetes. *Parasitol. Int.* **84**, 102407. https://doi.org/10.1016/j.parint.2021.102407 (2021).
34. Sala, K. A. et al. The plasmodium Berghei sexual stage antigen PSOP12 induces anti-malarial transmission blocking immunity both in vivo and in vitro. *Vaccine* **33**, 437–445. https://doi.org/10.1016/j.vaccine.2014.11.038 (2015).
35. MacDonald, N. J. et al. Structural and immunological differences in plasmodium falciparum sexual stage transmission-blocking vaccines comprised of Pfs25-EPA nanoparticles. *NPJ Vaccines.* **8**, 56. https://doi.org/10.1038/s41541-023-00655-5 (2023).
36. Kumar, V. et al. PHISTc protein family members localize to different subcellular organelles and bind plasmodium falciparum major virulence factor PfEMP-1. *FEBS J.* **285**, 294–312. https://doi.org/10.1111/febs.14340 (2018).
37. Murphy, S. C. et al. Erythrocyte detergent-resistant membrane proteins: their characterization and selective uptake during malarial infection. *Blood* **103**, 1920–1928 (2004).
38. Paone, S. et al. Characterization of the erythrocyte GTPase Rac1 in relation to plasmodium falciparum invasion. *Sci. Rep.* **10**, 22054. https://doi.org/10.1038/s41598-020-79052-0 (2020).
39. Mankelow, T. J., Satchwell, T. J. & Burton, N. M. Refined views of multi-protein complexes in the erythrocyte membrane. *Blood Cells Mol. Dis.* **49**, 1–10. https://doi.org/10.1016/j.bcmd.2012.03.001 (2012).
40. Lalle, M. et al. Dematin, a component of the erythrocyte membrane skeleton, is internalized by the malaria parasite and associates with plasmodium 14-3-3. *J. Biol. Chem.* **286**, 1227–1236. https://doi.org/10.1074/jbc.M110.194613 (2011).
41. Trager, W. & Jensen, J. B. Human malaria parasites in continuous culture. *Science* **193**, 673–675 (1976).
42. Rivadeneira, E. M., Wasserman, M. & Espinal, C. T. Separation and concentration of schizonts of plasmodium falciparum by Percoll gradients. *J. Protozool.* **30**, 367–370 (1983).
43. Lambros, C. & Vanderberg, J. P. Synchronization of plasmodium falciparum erythrocytic stages in culture. *J. Parasitol.* **65**, 418–420 (1979).
44. Ribaut, C. et al. Concentration and purification by magnetic separation of the erythrocytic stages of all human plasmodium species. *Malar. J.* **7**, 45. https://doi.org/10.1186/1475-2875-7-45 (2008).
45. Gupta, S. K., Schulman, S. & Vanderberg, J. P. Stage-dependent toxicity of N-acetyl-glucosamine to plasmodium falciparum. *J. Protozool.* **32**, 91–95. https://doi.org/10.1111/j.1550-7408.1985.tb03020.x (1985).
46. Carter, R. et al. Plasmodium falciparum: an abundant stage-specific protein expressed during early gametocyte development. *Exp. Parasitol.* **69**, 140–149. https://doi.org/10.1016/0014-4894(89)90182-3 (1989).

47. Di Girolamo, F. et al. Plasmodium lipid rafts contain proteins implicated in vesicular trafficking and signalling as well as members of the PIR superfamily, potentially implicated in host immune system interactions. *Proteomics* **8**, 2500–2513. https://doi.org/10.1002/pmic.200700763 (2008).
48. Folch, J., Lees, M. & Sloane Stanley, G. H. A simple method for the isolation and purification of total lipides from animal tissues. *J. Biol. Chem.* **226**, 497–509 (1957).
49. Blisnick, T. et al. Pfsbp1, a maurer's cleft plasmodium falciparum protein, is associated with the erythrocyte skeleton. *Mol. Biochem. Parasitol.* **111**, 107–121. https://doi.org/10.1016/s0166-6851(00)00301-7 (2000).
50. Ferreri, C. et al. Plasmalogens: free radical reactivity and identification of trans isomers relevant to biological membranes. *Biomolecules* **13** https://doi.org/10.3390/biom13050730 (2023).
51. Küçüksayan, E. et al. Sapienic acid metabolism influences membrane plasticity and protein signaling in breast cancer cell lines. *Cells* **11** https://doi.org/10.3390/cells11020225 (2022).
52. Vetica, F. et al. Free-Radical-Mediated formation of Trans-Cardiolipin isomers, analytical approaches for lipidomics and consequences of the structural organization of membranes. *Biomolecules* **10** https://doi.org/10.3390/biom10081189 (2020).
53. Silva, J. C., Gorenstein, M. V., Li, G. Z., Vissers, J. P. & Geromanos, S. J. Absolute quantification of proteins by LCMSE: a virtue of parallel MS acquisition. *Mol. Cell. Proteom.* **5**, 144–156. https://doi.org/10.1074/mcp.M500230-MCP200 (2006).
54. de Hoon, M. J., Imoto, S., Nolan, J. & Miyano, S. Open source clustering software. *Bioinformatics* **20**, 1453–1454. https://doi.org/10.1093/bioinformatics/bth078 (2004).
55. Shannon, P. et al. Cytoscape: a software environment for integrated models of biomolecular interaction networks. *Genome Res.* **13**, 2498–2504. https://doi.org/10.1101/gr.1239303 (2003).

Acknowledgements

Regione Lazio contributed to this study in the context of PhD programme "Dottorati di innovazione per le imprese" - DETERMINAZIONE DIRIGENZIALE N. G04110 DEL 05/04/2022 E RETTIFICA N. G04705 DEL 20/4/2022.

Author contributions

GS: methodology; software analysis; formal analysis; data curation. FF: methodology; data curation. CB: investigation. LM: software. SM: investigation. ML: investigation. SP: investigation. AO: investigation. CF: methodology. AS: methodology MP: conceptualization; validation; resources; writing – original draft; project administration CC: conceptualization; investigation; writing -review and editing; visualization EP: conceptualization; software; formal analysis; resources; writing – original draft; data curation; visualization; supervision; writing-review and editing.

Declarations

Competing interests

The authors declare no competing interests.

Additional information

Supplementary Information The online version contains supplementary material available at https://doi.org/10.1038/s41598-025-17908-z.

Correspondence and requests for materials should be addressed to C.C.